Corey Hebert
Scientific Computing: Final Project
8 May 2008

Variations on the Jumprope Assignment

Problem Overview

Imagine for a moment, a jumprope fixed at both ends and rotating in space. If simply left hanging, this rope would take the shape of a catenary due to the force of gravity pulling it downward; however, a much more interesting case is to examine the shape of the rope while it is spinning at some angular velocity. Additionally, the effects on the shape if the density of the rope is non-constant and if rope is elastic so that it can stretch are also of interest.

Setup and Equations

First, we will define the relevant parameters for the rope. The rope will have length L with one endpoint located at the origin, and the other at a distance H along the x-axis. The density of the rope will be given by the function $\rho(s)$ which relies upon a parameterization of the rope so that s varies lineraly from 0 at the origin to L at the far end of the rope. For the elastic case, we will use $k(s)$ to characterize the elasticity at various points along the rope; one can think of this as defining the spring constant as a function of the location along the rope. The angular velocity of the rope will be given by w.

To generate the equations for a rope, it is helpful to begin by looking at a free-body diagram for a small segment of the curve (fig. 1). Summing the red tension forces with the blue acceleration forces yields

$$\mathbf{x}_{tt}(s,t)\rho(s)\Delta s = -\mathbf{T}(s,t) + \mathbf{T}(s+\Delta s,t) + \mathbf{a}(s,t)\rho(s)\Delta s$$

which can be rewritten as

$$\mathbf{x}_{tt}(s,t)\rho(s) = \mathbf{T}_s(s,t) + \mathbf{a}(s,t)\rho(s), \qquad (1)$$

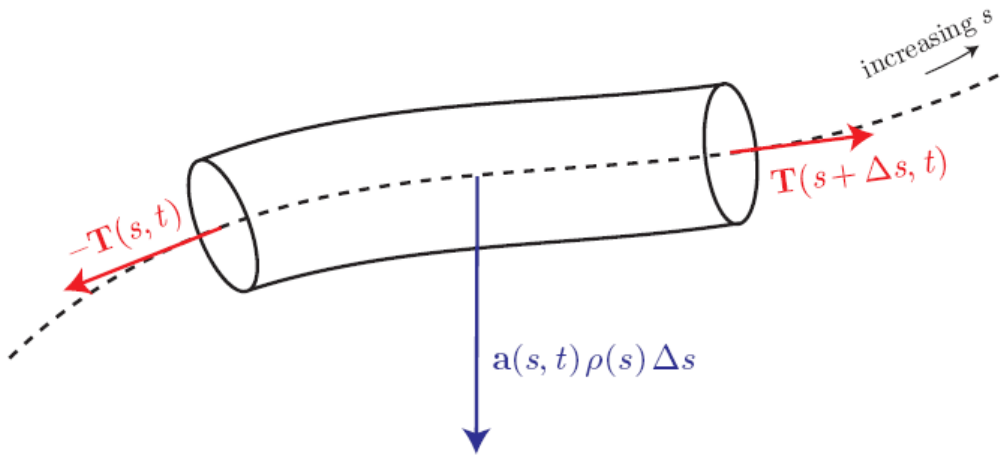

Fig. 1 *Free-body diagram of a small segment of the curve. The dashed curve is* $\mathbf{x}(s,t)$*, the centerline of the string, rope, or chain.*

the master wave equation. From this equation, two systems of equations can be derived that describe the shape of a rope with variable density that is either inextensible or extensible.

To generate equations for the extensible case we must look more closely at the tension forces present along the rope. We can rewrite this term as

$$\mathbf{T}(s,t) = T(s,t)\frac{\mathbf{x}_s(s,t)}{\|\mathbf{x}_s(s,t)\|}$$

where exactly how we define the term $T(s,t)$ controls the elastic properties of the rope. If $T(s,t) = E\|\mathbf{x}_s\|$, where E is known as Young's modulus, then the rope would be perfectly elastic. Instead of using this less realistic characterization of elasticity, one can use $T(s,t) = k\left(\|\mathbf{x}_s\| - 1\right)$ which makes the rope linearly elastic where k, again, can be thought of as the spring constant for the rope. At sufficiently high rotation rates, the dominant force in the system is a centripetal force which, in the rotating frame of reference, is given by $w^2 y(s)\rho(s)\Delta(s)\mathbf{j}$. Inserting this expression for $\mathbf{a}(s, t)$ in equation (1) yields

$$\mathbf{0} = \frac{\partial}{\partial s}\left(T(s)\frac{\mathbf{x}_s}{\|\mathbf{x}_s(s,t)\|}\right) + w^2 y(s)\rho(s)\mathbf{j}\,. \qquad (2)$$

Substituting for *T(s)* with the expression for linear elasticity yields

$$\mathbf{0} = \frac{\partial}{\partial s}\left(k(s)\mathbf{x}_s - k(s)\frac{\mathbf{x}_s}{\|\mathbf{x}_s\|}\right) + w^2 y(s)\rho(s)\mathbf{j}\,. \qquad (3)$$

Observing that $\mathbf{x}_s = x(s)\mathbf{i} + y(s)\mathbf{j}$ and that accordingly, $\|\mathbf{x}_s\| = \sqrt{(x')^2 + (y')^2}$, turns (3) into an increasingly messy multi-component system; this is further complicated when you integrate both the x-component and the y-component to remove the derivative. To handle these manipulations, Mathematica was used, and ultimately generated

$$\left\{\left\{x''[s] \to \frac{-\text{omega}^2\ \text{rho}\ y[s]\ x'[s]^2 + k'[s]\ \left(y'[s]^3 - x'[s]\ y'[s]^2\sqrt{x'[s]^2+y'[s]^2} - x'[s]^3\left(-1+\sqrt{x'[s]^2+y'[s]^2}\right)\right)}{k[s]\ \left(x'[s]\ y'[s] + y'[s]^2\sqrt{x'[s]^2+y'[s]^2} + x'[s]^2\left(-1+\sqrt{x'[s]^2+y'[s]^2}\right)\right)},\right.\right.$$

$$\left.\left.y''[s] \to -\frac{\text{omega}^2\ \text{rho}\ y[s]\ \left(x'[s]\ y'[s] + x'[s]^2\sqrt{x'[s]^2+y'[s]^2} + y'[s]^2\sqrt{x'[s]^2+y'[s]^2}\right) + k'[s]\ y'[s]\ \left(x'[s]\ y'[s] + x'[s]^2\left(-2+\sqrt{x'[s]^2+y'[s]^2}\right) + y'[s]^2\left(-1+\sqrt{x'[s]^2+y'[s]^2}\right)\right)}{k[s]\ \left(x'[s]\ y'[s] + y'[s]^2\sqrt{x'[s]^2+y'[s]^2} + x'[s]^2\left(-1+\sqrt{x'[s]^2+y'[s]^2}\right)\right)}\right\}\right\}$$

as the equations for x'' and y'', where rho is $\rho(s)$ and omega is w. These equations are used with a shooting method to find the shape of the rotating rope.

In the inextensible case, one starts from equation (2) and assumes that $\|\mathbf{x}_s(s,t)\| = 1$ holds; this particular case allows the examination of the effects of variable-density, independent of elasticty. For ease of representation and computation, (2) can be modified by substituting for x_s and y_s with $\cos(\theta(t))$ and $\sin(\theta(t))$, respectively; this has the added benefit of ensuring the inextensibility constraint is satisfied since it forces $\|\mathbf{x}_s(s,t)\|$ to be 1. The substitution yields

$$0 = \frac{\partial}{\partial s}\left[T(s)\cos(\theta)\right]$$

$$0 = \frac{\partial}{\partial s}\left[T(s)\sin(\theta)\right] + w^2\rho(s)\int_0^s \sin(\theta(\tau))d\tau$$

for the two components. From the first equation we can find an expression for the tension, $T(s) = \frac{C}{\cos(\theta)}$, and substitute it into the second to acquire the nonlinear equation

$$0 = \frac{C\theta'(s)}{\rho(s)\cos^2(\theta(s))} + w^2 \int_0^s \sin(\theta(\tau))d\tau .$$

Differentiating this and dividing into a system of equations yields

$$x' = \cos\theta$$
$$y' = \sin\theta$$
$$\theta'' = -2(\theta')^2 \tan\theta + \frac{\rho'(s)}{\rho(s)} - \frac{w^2\rho(s)}{C}\sin\theta\cos^2\theta$$

which, when subject to the boundary conditions $x(0) = 0$, $x(L) = H$, $y(0) = 0$, $y(L) = 0$, and $\theta'(0) = 0$, can be used to find the shape of an inextensible rope with variable density by the shooting method.

Each of the two sets of equations was coded up in Matlab. To run, a variety of parameters were required to be set including *w*, *L*, and *H*. In addition, both required an initial guess for two of their parameters: C and θ' for the inextensible case, and x" and y" for the extensible case. From these initial guesses, the code attempted to solve for the shape of the rope via the shooting method, limited to 10000 iterations. In many cases, the code was unable to converge on a solution, so many trials were necessary to find suitable combinations of initial conditions that yielded an interesting rope shape.

Results

The results here presented build upon my work for assignment 4 in which I concluded that both the tension and the angular velocity could effect how many modes a given inextensible rope displayed and furthermore that the tension was dependent upon the length of the rope and

the distance between the fixed points. Generally, here, density and elasticity were explored while minding these other constraints – notably, keeping them constant across trials as much as possible.

The density of the rope was varied to see what effects this had on the shape of the rope. Two variant density functions were used: a linear function which increased from one end to the other and a sinusoidal function which was used to place "weights" along the rope in various places to observe the behavior. Interestingly, the variable density caused some unusual shapes. One might expect that a normally distributed density would cause a symmetric response in the rope. However, as figures 2, 3, and 7 show, even though the density is normally distributed, the apparently stable shape of the rope is not necessary something that matches our intuition; repeated tests shooting with these parameters converge similarly. Considering the linearly dense ropes, it is interesting to observe that, in figures 4 and 5, the more dense sections of the rope are apparently more stable near the axis of rotation; one supposes that there is an element of conservation between the angular velocity and the relative masses that accounts for this. Additionally, it was again observed that changes in the tension would have an effect on the shape of the rope even if the density was not constant; this can be seen in figures 4, 5, and 6.

In the case of the elasticity, in the simple cases it is clear that the stretching of the rope has a noticeable effect on the shape of the rope – namely, it causes the center of the rope to extend further then the inelastic case. Furthermore, if the elasticity of the rope is higher, this effect is less pronounced. In both cases, these observations match general expectations. Another observation that may be less obvious, but seems quite reasonable physically, is the fact that the stretching is not uniform along the rope; there is more stretching near the fixed points than in the middle. Since there is a larger amount of rope (in terms of mass, for a uniform density rope)

pulling outward when you view things from a point near the end, this seems reasonable to explain why more stretching occurs at these points near the end.

Conclusions

Ultimately, the experimentation with density and elasticity demonstrated that this is definitely a computationally intensive problem. Furthermore, it produced some interesting results which, without physical experimentation, one is left to wonder whether or not the modeled results actually match what one would see in the real world. However, there certainly are enough results that make intuitive sense to indicate that, at least in some cases, the model used is, or at least seems to be, correct.

Sources

Yong, Darryl. "Strings, Chains, and Ropes." *Society for Industrial and Applied Mathematics* Vol. 48, No. 4, pp 771-781.

Additional inspiration and confirmation from a presentation by: Melissa Strait

Figures

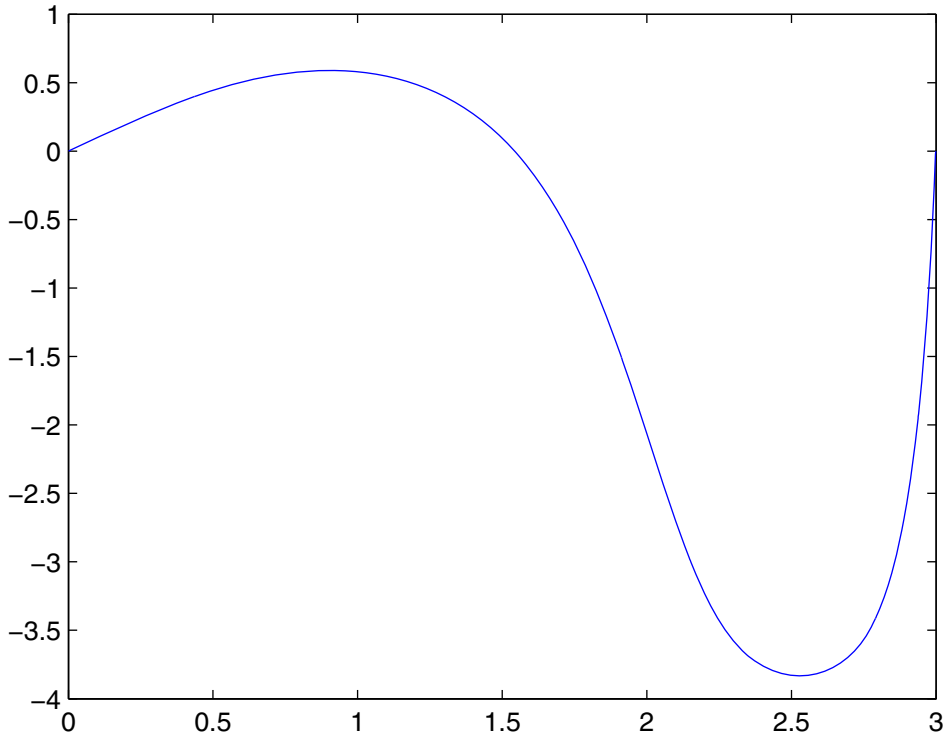

Figure 2:

```
>> script(2, @(s) sin(s*pi/10)+1, @(s) (pi/10)*cos(s*pi/10)+1, 3, 10, [1.2; 1])
Optimization terminated: first-order optimality is less than options.TolFun.

x =

   0.779842902558538
   2.761641886211272


fval =

  1.0e-007 *

  -0.467420657734863
   0.097856102665439
```

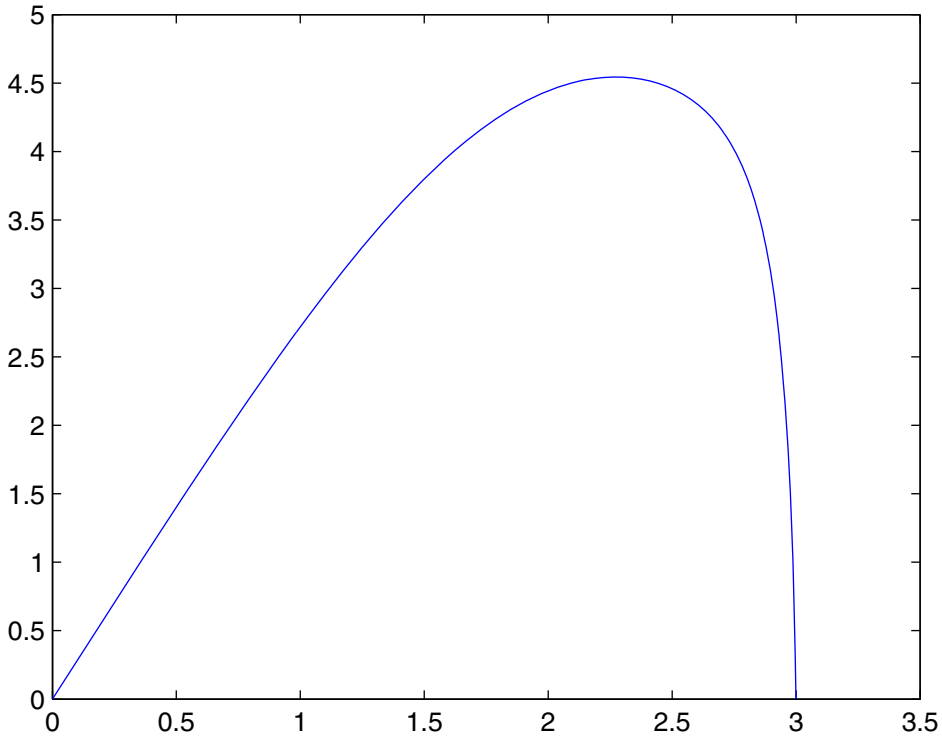

Figure 3:

```
>> script(10, @(s) abs(sin(s*pi/5))+1, @(s) (pi/10)*abs(cos(s*pi/5))+1, 3, 10, [2; 600])
Optimization terminated: first-order optimality is less than options.TolFun.

ans =

  1.0e+003 *

   0.001230335943632  -0.000000000000044
   3.434546702096819  -0.000000000000085
```

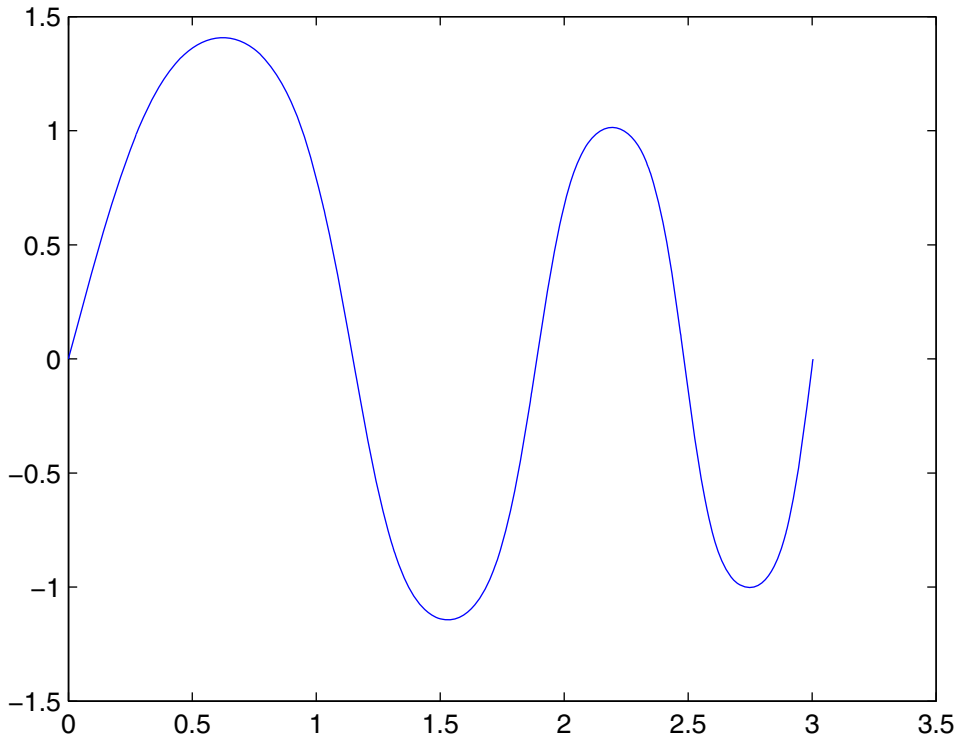

Figure 4:

```
>> script(10, @(s) s+1, @(s) 1, 3, 10, [2; 60])
Optimization terminated: norm of relative change in X is less
 than max(options.TolX^2,eps) and  sum-of-squares of function
 values is less than sqrt(options.TolFun).

ans =

   1.328865264512805   0.003592518871093
  61.947033302374741  -0.000687400115341
```

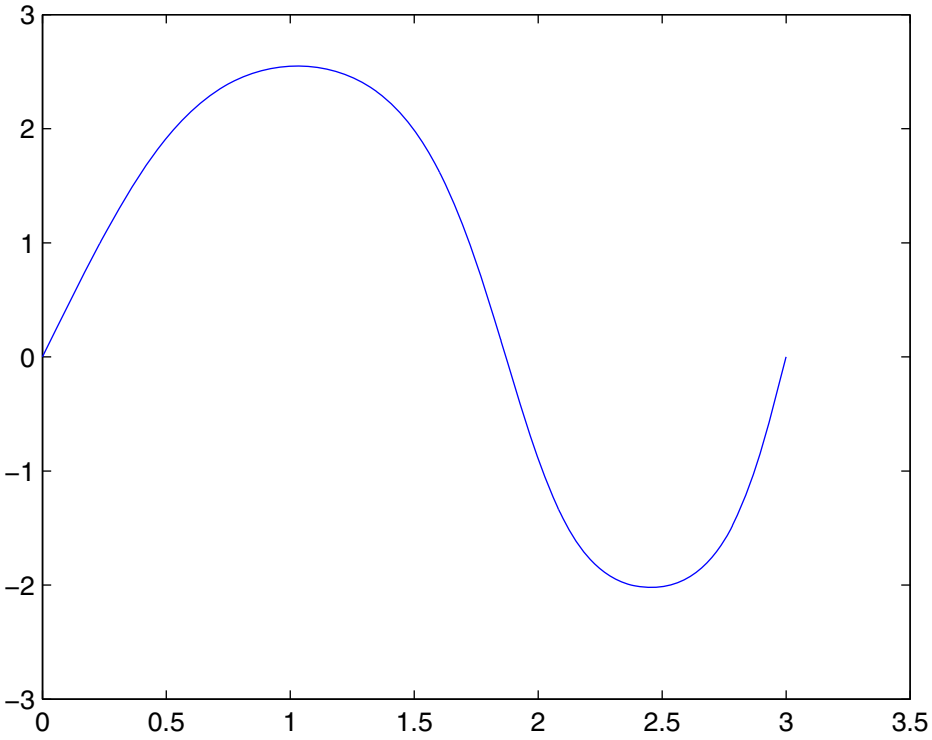

Figure 5:

```
>> script(10, @(s) s+1, @(s) 1, 3, 10, [2; 300])
Optimization terminated: first-order optimality is less than options.TolFun.

ans =

  1.0e+002 *

   0.013470298123734   0.000000000042472
   2.566461956142275  -0.000000000009162
```

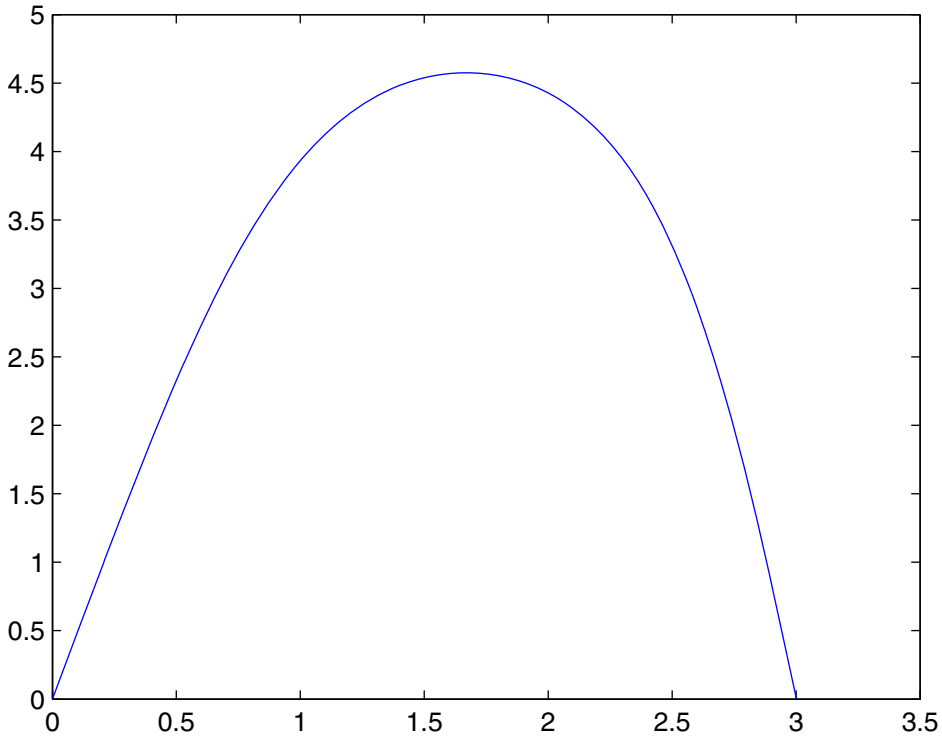

Figure 6:

```
>> script(10, @(s) s+1, @(s) 1, 3, 10, [2; 1200])
Optimization terminated: norm of relative change in X is less
 than max(options.TolX^2,eps) and  sum-of-squares of function
 values is less than sqrt(options.TolFun).

ans =

  1.0e+003 *

   0.001367290443937   0.000001181611726
   1.100985398907829   0.000000225817767
```

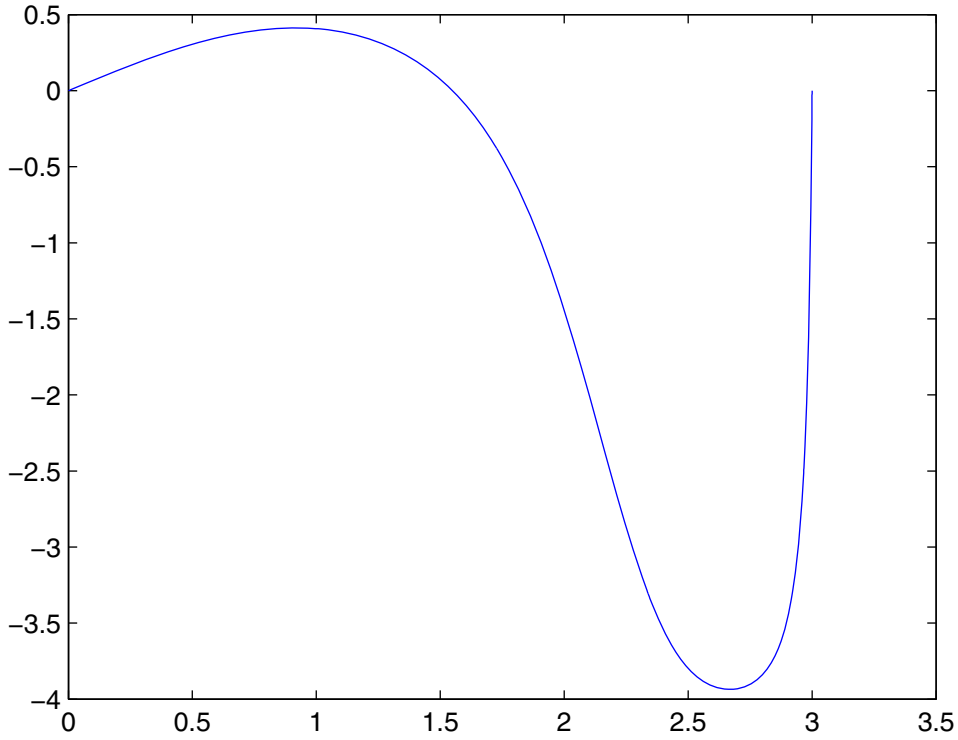

Figure 7:

>> script(10, @(s) abs(sin(s*pi/5+2.5))+1, @(s) (pi/10)*abs(cos(s*pi/5+2.5))+1, 3, 10,

[2; 60])
Optimization terminated: first-order optimality is less than options.TolFun.

ans =

```
  0.597139945602211  -0.000000000022425
 80.566095534824612   0.000000000251374
```